Environmental Health Perspectives
Vol. 15, pp. 147-156, 1976

Factors Influencing the Deposition of Inhaled Particles*

by H. C. Yeh,† R. F. Phalen,‡ and O. G. Raabe§

Because the initial deposition pattern of inhaled particles of various toxic agents determines their future clearance and insult to tissue, respiratory tract deposition is important in assessing the potential toxicity of inhaled aerosols.

Factors influencing the deposition of inhaled particles can be classified into three main areas: (1) the physics of aerosols, (2) the anatomy of the respiratory tract and (3) the airflow patterns in the lung airways. In the physics of aerosols, the forces acting on a particle and its physical and chemical properties, such as particle size or size distribution, density, shape, hygroscopic or hydrophobic character, and chemical reactions of the particle will affect the deposition. With respect to the anatomy of the respiratory tract, important parameters are the diameters, the lengths, and the branching angles of airway segments, which determine the deposition. Physiological factors include airflow and breathing patterns which influence particle deposition. Various lung models used in predicting particle deposition are reviewed and discussed. The airway structures of various animal species are compared, showing the unique structure of the human lung compared to the animal species under study. Regional deposition data in man and dog are reviewed. Recent deposition data for small rodents are presented, showing regional difference in deposition with the right apical lobe having the highest relative deposition.

Introduction

Knowledge of the patterns of initial deposition of inhaled particles of various toxic agents, including radionuclides, within the respiratory tract is essential for determining future clearance and dose patterns, and, therefore, is important in assessing the potential toxicity associated with these particles. Many factors will influence the deposition of inhaled particles, among which the more important are: (1) the physics of aerosol particles, (2) the anatomy of the respiratory tract and (3) respiratory physiology. These factors are discussed in this paper.

Physics of Aerosol Particles

An aerosol can be defined as a system of solid or liquid particles which are (a) dispersed in a gaseous medium, (b) able to remain suspended in the gaseous medium for a long time relative to the time scale of interest, i.e., are relatively stable; and (c) have a high surface area to volume ratio. The geometrical diameters of aerosol particles normally fall within the range between 0.001 and 100 μm. For a spherical particle, particle size is defined as the geometrical (real) diameter. For nonspherical particles, particle size may be defined as shown in Figure 1, with the projected area diameter D_p commonly used as the (equivalent) geometrical diameter. Two other important conventions for describing particle sizes are frequently used in aerosol science; namely, the Stokes' (equivalent) diameter and the aerodynamic (equivalent) diameter. These are de-

* This paper was presented at the 102nd American Public Health Association Annual Meeting, New Orleans, Louisiana, October 20-24, 1974.

† Inhalation Toxicology Research Institute, Lovelace Foundation, P.O. Box 5890, Albuquerque, New Mexico 87115.

‡ Present address: Department of Community and Environmental Medicine, College of Medicine, University of California at Irvine, Irvine, California 92664.

§ Present address: Radiobiology Laboratory, University of California at Davis, Davis, California 95616.

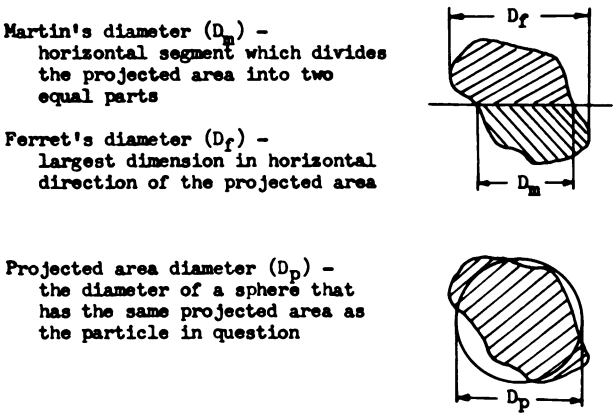

FIGURE 1. Definitions of nonspherical particle geometrical sizes.

fined as follows: Stokes' diameter is that diameter of a sphere that has the same density and terminal settling velocity as the nonspherical particle in question; the aerodynamic (equivalent) diameter is the diameter of a unit density (one g/cm³) sphere that has the same terminal settling velocity as the subject particle.

Actually, particles come in a range of sizes, and an aerosol is described by a size distribution. Usually, such a distribution can be satisfactorily represented by a lognormal function and described by the geometric mean and geometric standard deviation. Figure 2 shows a lognormal distribution of particles with some of its

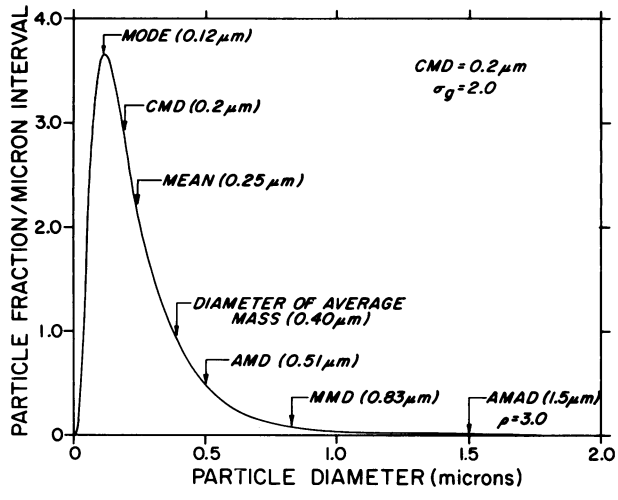

FIGURE 2. Lognormal distribution of particles with a geometric mean of 0.2 μm and geometric standard deviation of 2.0.

associated parameters, including count median diameter (CMD), (surface) area median diameter (AMD), mass median diameter (MMD) and activity median aerodynamic diameter (AMAD) for a distribution of radioactive particles whose physical density is 3 g/cm³. Depending on application, one of these parameters with associated geometric standard deviation σ_g can be used to describe the aerosol. For example, if mass is of interest, then MMD can be used. Likewise, for radioactive aerosols, AMAD is more suitable.

Figure 3 illustrates three main mechanisms which cause particle deposition in the lung. The first mechanism is called inertial impaction. Since particles have a finite mass, individual particles may not follow the curvature of the air streamlines, due to their inertia, and may impact (hit

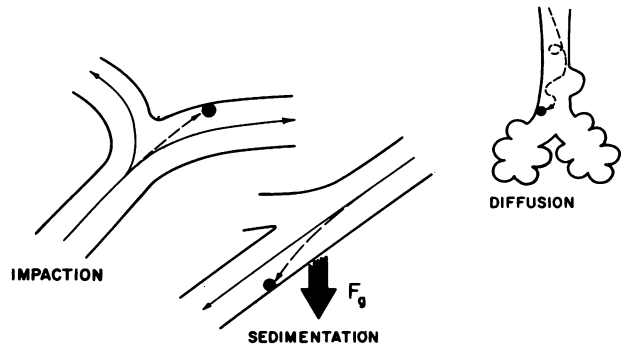

FIGURE 3. Three particle deposition mechanisms occurring within the respiratory tract.

and stick) on the wall of the airways. The second mechanism, sedimentation, is due to the gravitational force acting on a particle; it may settle and deposit on the lower surface of an airway. The third mechanism is called diffusion. When the particle size is small, random (Brownian) motion of a particle caused by the interaction of air molecules may cause it to move across the air streamlines and to deposit upon contact with the airway wall. There are some other mechanisms, such as interception and electrostatic charge associated with particles, which may be important in some cases. Interception is due to the physical size of the particle, making direct contact with the airway wall within the distance from the wall equal to particle radius. Since the particle size of interest in deposition is less than 6 or 10 μm in diameter compared with the smallest airway size of about 100 μm and larger, this mechanism is usually neglected, except when

dealing with aerosols of fibers which are too long to negotiate the bends in the respiratory tract. Electrostatic charge associated with particles may enhance deposition, due to electrical attraction. It is generally believed that this mechanism is important only in the nasal hair region and only when aerosols are highly charged; therefore, it is also neglected in most studies. Particle depositions in a tube (laminar flow) caused by diffusion, sedimentation, and impaction (P_D, P_S, P_I, respectively) are described by eqs. (1)-(3):

$$P_D = 4.07\varepsilon^{2/3} - 2.4\varepsilon - 0.446\varepsilon^{4/3} + \ldots \quad (1)$$

where

$$\varepsilon = LD/2R^2\bar{v} < 0.0156$$

and L is tube length, D is diffusion coefficient of particles, R is tube radius, and $\bar{v}$ is mean flow velocity;

$$P_S = 1 - \exp\left\{\frac{-4gC\varrho_p r_p^2 L\cos\phi}{9\pi\mu R\bar{v}}\right\} \quad (2)$$

where C is the Cunningham slip correction, ϱ_p is particle density, r_p is particle radius, ϕ is the inclination angle of the tube, and μ is fluid viscosity;

$$P_I = 1 - \frac{2}{\pi}\cos^{-1}(\theta S_t) + \frac{1}{\pi}\sin 2\cos^{-1}(\theta S_t) \quad (3)$$

where $S_t = C\varrho_p r_p^2\bar{v}/9\mu R$ and θ is banding angle.

Figure 4 shows how these three main mechanisms influence the deposition as a function of particle size and density for a given tube and flow velocity. Other physical or chemical properties of aerosols, which may influence the deposition, are the hygroscopic or hydrophobic character of the particle, gas-particle interactions, and chemical reactions which form a particle and cause its growth.

Anatomy of the Respiratory Tract

The lung is a very complex organ, and its exact anatomy has not been well-established. Because of the complexity of the lung structure, theoretical or experimental studies of particle deposition in a model lung have used some fairly simple lung models. For simplicity, the structure of the respiratory tract can be considered as a series of tubes connected together by successive branches from the trachea down to the respiratory bronchioles. The deposition equations (1)-(3) indicate that the key geometrical parameters of airway structure which relate to particle deposition are the airway segment lengths, diameters, inclinations to gravity, and branching angles. Unfortunately, existing lung models supply only part of

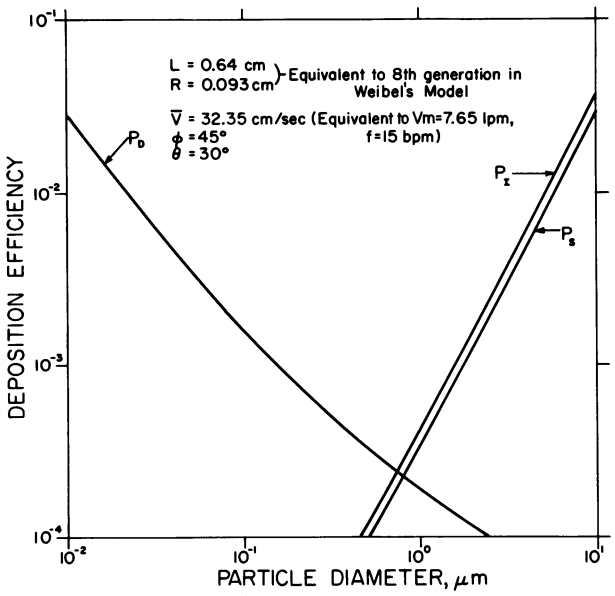

FIGURE 4. Deposition efficiencies in a tube with laminar flow (lpm=liters/minute; bpm=breaths/minute).

the needed information. Of the existing lung models (*1-8*), Weibel's (*4*) and Horsfield's (*5*) human lung models are based on extensive morphometric studies, while models of Findeisen (*1*), Landahl (*2*), and Davies (*3*) were developed more abstractly. With the exception of Horsfield's model, these models are symmetric and ordered generation by generation in a treelike manner. Table 1 shows Weibel's human lung model (*4*) of regular dichotomy, a model commonly used in physiological and deposition studies by many investigators. A characteristic of this lung model is the regular and symmetrical branching of the airways from the trachea through to the alveolar sacs, i.e., a parent segment branches into two daughter segments with equal diameters and equal branching angles. This type of lung model is oversimplified and does not have the characteristics of a true lung. On the other hand, Horsfield's model (*5*) is asymmetric in branching, but can be somewhat confusing and therefore may be difficult to use.

Lung morphometry has been studied for several years at the Inhalation Toxicology Research Institute. Our interest is in quantitating the geometry of the tracheobronchial tree in man, dog, rat and hamster. To this end, replica casts of silicone rubber have been carefully prepared for detailed trimming and hand measurement (*9*). Figure 5 shows two rat casts, one before and one after trimming.

Table 1. Weibel's human lung model (regular dichotomy).

Generation Z	Number per generation $n(Z)$	Diameter $d(Z)$, cm	Length $l(Z)$ cm
0	1	1.8	12.0
1	2	1.22	4.76
2	4	0.83	1.90
3	8	0.56	0.76
4	16	0.45	1.27
5	32	0.35	1.07
6	64	0.28	0.90
7	128	0.23	0.76
8	256	0.186	0.64
9	512	0.154	0.54
10	1024	0.13	0.46
11	2048	0.109	0.39
12	4096	0.095	0.33
13	8192	0.082	0.27
14	16384	0.074	0.23
15	32768	0.066	0.20
16	65536	0.060	0.165
17	131072	0.054	0.141
18	262144	0.050	0.117
19	524288	0.047	0.099
20	1048576	0.045	0.083
21	2097152	0.043	0.070
22	4194304	0.041	0.059
23[a]	8388608	0.041	0.050*

[a] Adjusted for complete generation.

Before presenting some of our morphometric data, some terminology must be addressed. Figure 6 shows an idealized model of an airway branch. The branch consists of three airway tubes. The first tube, the parent, divides into two

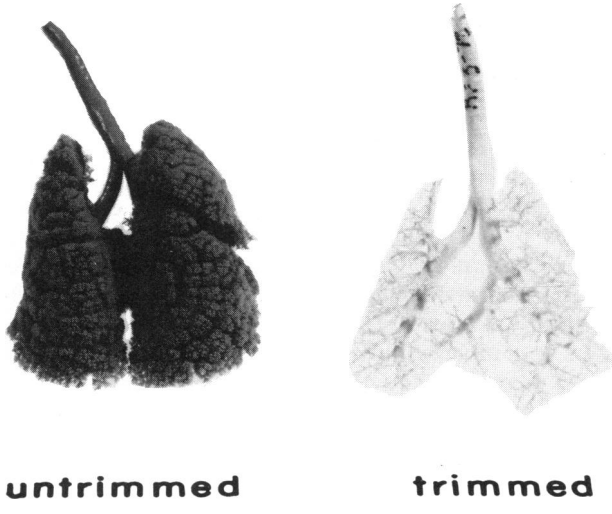

FIGURE 5. Trimmed and untrimmed silicone rubber casts of rat lung airways.

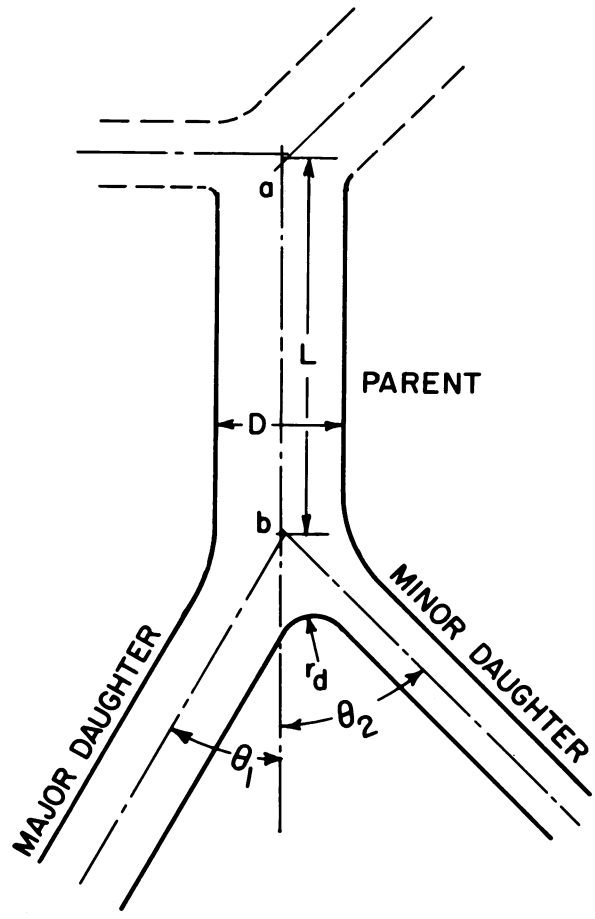

FIGURE 6. Idealized airway branch.

daughter segments. The major daughter has a larger diameter than the minor daughter by definition. The subscripts 1 and 2 are used to denote major and minor daughter segments, respectively.

Early data are summarized in Table 2 and Figure 7. These data were obtained from direct hand measurements on the casts, using a seven-power hand-held magnifier-comparater; the idealized model of an airway branch (Fig. 6), was used as a guide. Table 2 shows species differences in lung structure for various parameters. Not only is the lung structure asymmetric ($\theta_1 \neq \theta_2$, $D_1 \neq D_2$, $L_1 \neq L_2$), but also the human lung differs from the other three mammalian species, in that the human lung is more dichotomous whereas the other three species are monopodial with small branches branching out from larger branches. The dependence of branch angles and segment diameters on the diameter of the parent segment

Table 2. Species differences in lung structure (mean ± standard deviation of the mean).[a]

Species	n[b]	Branching angle		Tube diameter ratios		Length/diameter ratios	
		θ_1	θ_2	D_1/D_p	D_2/D_p	L_1/D_1	L_2/D_2
Human[c]	250	44 ± 1	55 ± 1	0.89 ± 0.01	0.73 ± 0.01	2.4 ± 0.07	2.7 ± 0.07
Beagle[d]	650	10 ± 1	58 ± 1	0.89 ± 0.01	0.62 ± 0.01	1.1 ± 0.02	1.9 ± 0.03
Rat	2510	13 ± 0.04	56 ± 0.03	0.87 ± 0.00	0.58 ± 0.00	1.4 ± 0.00	1.9 ± 0.00
Hamster[e]	630	17 ± 0.2	56 ± 0.1	0.89 ± 0.00	0.63 ± 0.00	1.4 ± 0.00	1.7 ± 0.00

[a] θ_1 and θ_2 are branching angles of major and minor daughters, respectively; D_p, D_1, and D_2 are tube diameters of parent, major daughter, and minor daughter, respectively; L_1 and L_2 are tube length of major and minor daughter, respectively.
[b] Number of airway segments being measured.
[c] Right apical lobe only.
[d] Right diaphragmatic lobe only.
[e] Right lung only.

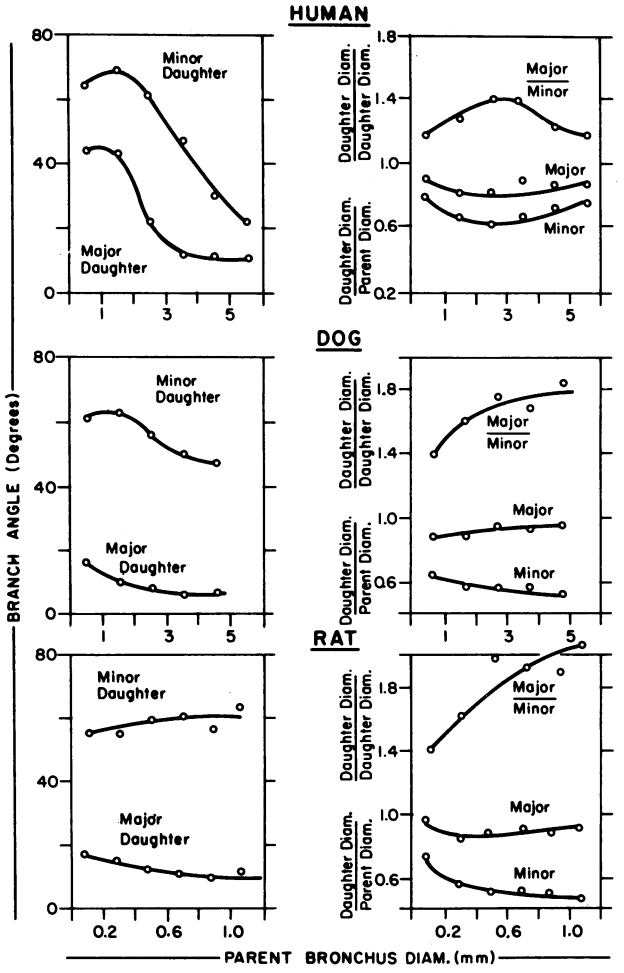

FIGURE 7. Dependence of airway anatomy on size of the bronchi.

is shown in Figure 7. In man and dog, branch angles for both major and minor daughters increase as one progresses distally down the tracheobronchial tree. In the rat, θ_1 increases and θ_2 decreases with decreasing parent diameter. Table 3 shows the average number of divisions and average path lengths between the trachea and terminal bronchioles for various lung lobes in rat and hamster. These structural differences between lobes may explain the uneven deposition of particles in the lobes in the animal experiments which is discussed later.

Air Flow in the Lung Airways

Gas flow inside the tracheobronchial tree is a very complicated phenomenon. Assuming the breathing flow rate is 20 l./min for man at rest, the Reynolds' number ($N_{Re} = \varrho u d/\mu$, where ϱ is density of the air, u is mean velocity, d is tube diameter, and μ is viscosity of the air) in various airway segments has been estimated (*10*) to range from 0.002 to 1670. From theoretical considerations, the flow should be laminar through-

Table 3. Average number of divisions and average path lenths between trachea and terminal bronchioles for various lung lobes in Long Evans Blu-LE rat and Syrian hamster.

Lung lobe[a]	Black and white hooded rat		Syrian hamster	
	Number of divisions	Path length, mm	Number of divisions	Path length, mm
Right lung				
RA	13	55.1	11	39.5
RC	15	62.9	13	46.5
RD	20	69.3	18	50.5
RI	17	65.1	15	48.4
Left lung	14	64.3	15	51.3

[a] RA = right apical lobe; RC = right cardiac lobe; RD = right diaphragmatic lobe; RI = right intermediate lobe.

out the airways, because the Reynolds' number in each segment of the airway is less than the critical Reynolds' number of about 2300 for normal breathing. But due to the influence of the larynx and bifurcations, the air flow in human lungs will be turbulent in some segments. West (*11*) observed gas flow in the upper bronchial tree in a hollow lung cast and reported that the flow is probably turbulent in the first few divisions. Martin and Jacobi (*12*) concluded from their study that no laminar air flow exists in the trachea and larger bronchi. Schroter and Sudlow (*13*) studied the flow patterns in models of the human bronchial airways and reported that secondary flow exists at bifurcations and that flow profiles were highly asymmetric about the center axis at all flow rates. From these findings, one may reasonably assume that the air flow is probably turbulent with secondary flow in larger airways and is laminar in small airways where Reynolds' numbers are small. Turbulent flow will enhance the deposition due to diffusion.

Because of the complicated nature of the airflow inside the airways, no analytical equations have been obtained to express exact flow characteristics inside the lung. In predicting particle deposition, it is usually assumed that the flow is laminar. Under the assumption of laminar flow, the flow velocity in airways will affect the deposition efficiency such that increasing flow velocity, increases deposition due to impaction while decreasing deposition due to diffusion and sedimentation. Breathing volume and frequency will determine the mean flow velocity in each airway segment; therefore, the breathing pattern is a key physiological factor in influencing the deposition of inhaled particles. The effect of breathing pattern is illustrated in Figure 8. This figure is based on the International Commission for Radiological Protection (ICRP) lung model (*14*) for tidal volumes of 750 and 2150 ml at 15 breaths/min.

Regional Deposition

The term, total deposition, is defined as the ratio of the number or mass of particles deposited in the respiratory tract to the number or mass of particles inhaled. Alveolar deposition, sometimes called pulmonary deposition, is defined as the ratio of the number or mass of particles deposited in the pulmonary region to the number or mass of particles inhaled. Lobar deposition is defined as the ratio of number or mass of particles deposited in each lobe of the lung to the number or mass of particles inhaled. Most experimental deposition

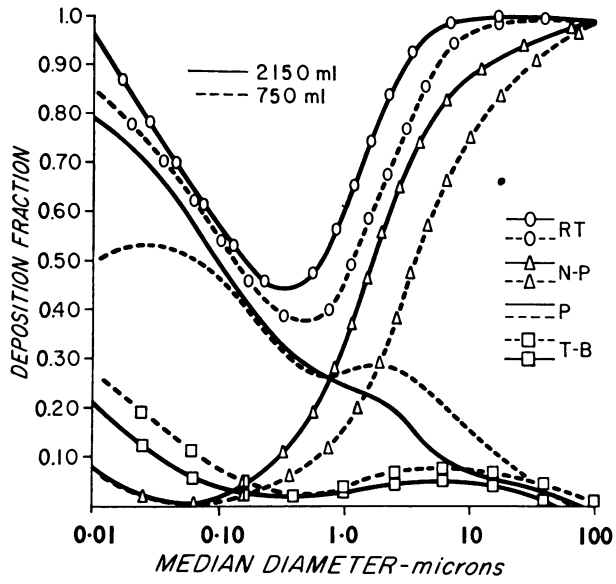

FIGURE 8. Calculated average deposition curves for two ventilatory rates for lognormally distributed aerosols of various mass median aerodynamic diameters, i.e., 750 ml and 2150 ml tidal volumes, 15 breaths/min.: (RT) total for respiratory tract; (NP) nasopharyngeal; (TB) tracheobronchial; (P) pulmonary. From Task Group on Lung Dynamics (*14*) reproduced with permission of Pergamon Press.

studies in man and experimental animals are focused on total deposition with relatively few attempts made to measure regional particle deposition. Unfortunately, due to uncontrolled experimental variables and poor experimental techniques in most studies, the availability of good data is limited.

The Task Group on Lung Dynamics of the International Commission on Radiological Protection (ICRP) made careful calculations of the expected deposition in the human respiratory tract of particles of various aerodynamic equivalent sizes and of lognormally distributed aerosol distributions (*14*). The Task Group defined three functional compartments for the respiratory tract: (1) the nasopharynx (NP) from the anterior nares to the level of the larynx or epiglottis, (2) the tracheobronchial region (TB) from the trachea down to the terminal bronchioles and included all ciliated bronchioles, and (3) the pulmonary region (P) or parenchyma of the lung including respiratory bronchioles, alveolar ducts and alveoli. The Task Group used the empirical equation of Pattle (*15*) for calculating deposition in the NP region and the anatomical model and general method of Findeisen (*1*) for calculating TB and P deposition. Diffusional deposition in the

lung was calculated by using the Gormley-Kennedy (*16*) equation for diffusional deposition in cylindrical tubes. The results of their calculations for three different breathing patterns were compared to available deposition data for man up to 1965, and found to be in general agreement, although the scatter of the available data was large. With the calculated deposition fractions for particle sizes at 15 respirations/min and 1450 ml-min volume, the predicted deposition of various lognormally distributed aerosols was also calculated. It was discovered that lognormal aerosols with the same mass median aerodynamic diameter had very similar predicted deposition mass fractions in the three functional compartments of the respiratory tract. The average value of the calculated deposition for various lognormally distributed aerosols from the Task Group report is shown in Figure 8 as deposition fraction versus aerosol mass median aerodynamic diameter for two different minute volumes.

Figures 9 and 10 show the human deposition data summarized by Lippmann (*17*). Also included are curves for mouth breathing calculated

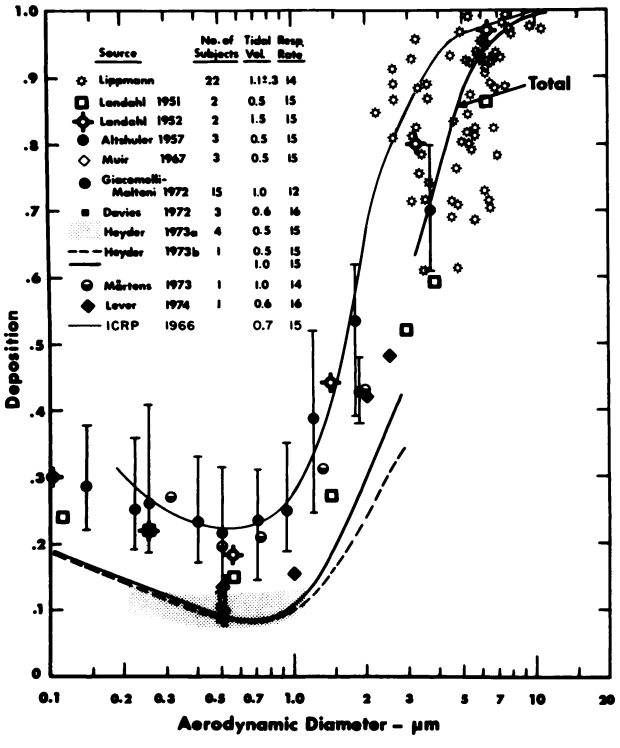

FIGURE 9. Summary of human deposition data (mouth breathing). Adapted from Lippmann (*17*) with permission of the publisher.

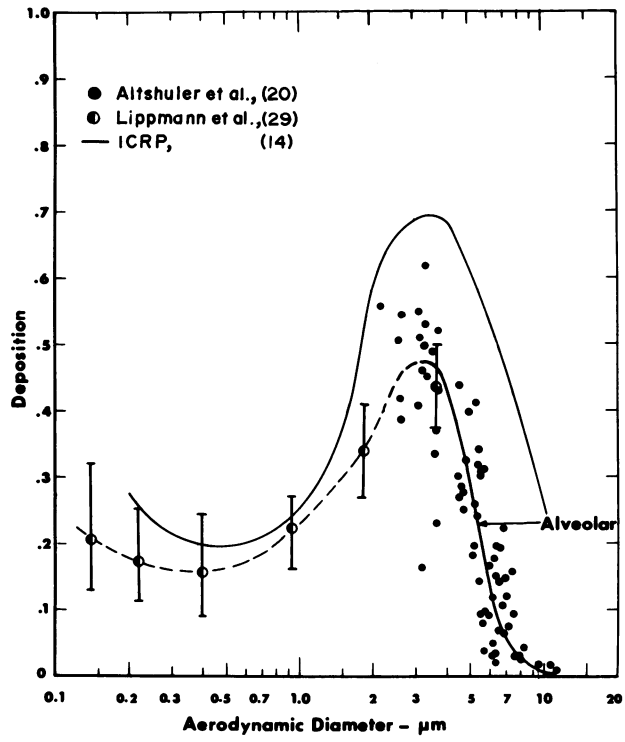

FIGURE 10. Human deposition data in pulmonary region. From Lippmann (*17*) with permission of the publisher.

upon the regional deposition predicted by the Task Group on Lung Dynamics of the ICRP (*14*). The total respiratory tract deposition with mouth breathing is shown in Figure 9. Considerable variation exists among the subjects and within each subject. Nevertheless, the data indicate a minimum of deposition at about 0.5 μm aerodynamic diameter. Figure 10 shows alveolar deposition data of Altshuler et al. (*28*) and Lippmann et al. (*29*) as a function of particle size. The decrease in particle deposition for larger particles does not mean low deposition efficiency in the pulmonary region, but rather that only a fraction of the larger particles reach the pulmonary region because they deposit in the upper airways. There is a maximum pulmonary deposition at about 3 μm for mouth breathing. Also, the ICRP curve predicts higher pulmonary deposition. Figure 11 shows the pulmonary deposition of radiolabeled polydisperse aerosols inhaled by the Beagle dog (*30*). Dashed lines indicate the estimated boundaries of the data. The solid line represents the pulmonary deposition in man according to the ICRP Task Group (*14*).

Some results from small rodent inhalation

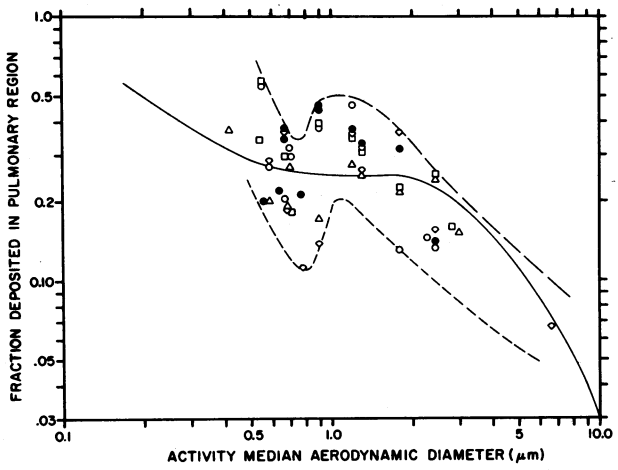

FIGURE 11. Pulmonary deposition of ^{140}La-labeled polydisperse aerosols inhaled by beagle dogs. Various symbols indicate individual dogs. From Cuddihy et al. (*30*) with permission of Pergamon Press.

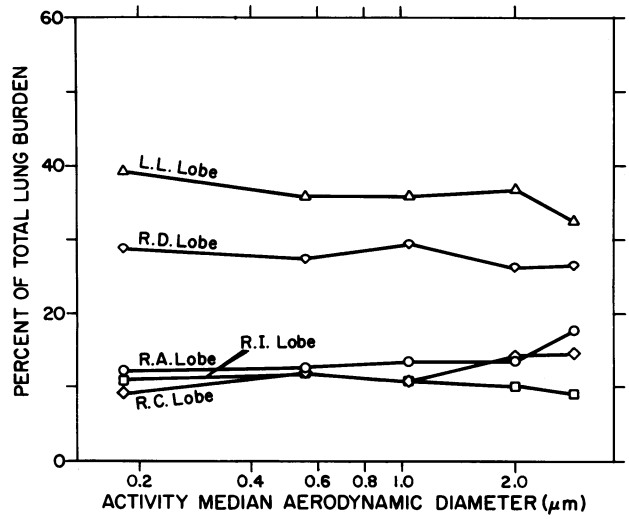

FIGURE 13. Relative lobar deposition of ^{169} Yb in fused aluminosilicate spheres in Syrian hamsters.

studies recently conducted at the Inhalation Toxicology Research Institute (*31*) are shown in Figures 12-15. Figures 12 and 13 show the relative lobar deposition of monodisperse or near-monodisperse radiolabeled fused aluminosilicate spheres in rats and hamsters, respectively. On the average, the activity (or number of deposited particles) within the right lung was about twice that of the left lung. Furthermore, approximately 40-45% of the activity of the right lung was in the right diaphragmatic lobe. Figures 14 and 15 show the lobar deposition data expressed as a percentage of total lung burden per percentage of total lung weight. This is equivalent to the normalized activity concentration in the lung lobes. The right apical lobe most frequently had the highest concentration of deposited particles (except in the case of < 0.2 μm in the hamster). For the other four lobes, the relative concentration varied with particle size. Also, the relative concentrations were more even (less

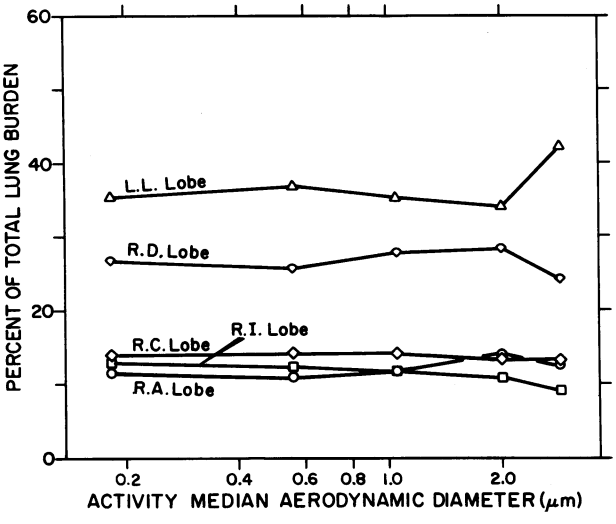

FIGURE 12. Relative lobar deposition of ^{169} Yb in fused aluminosilicate spheres in rats.

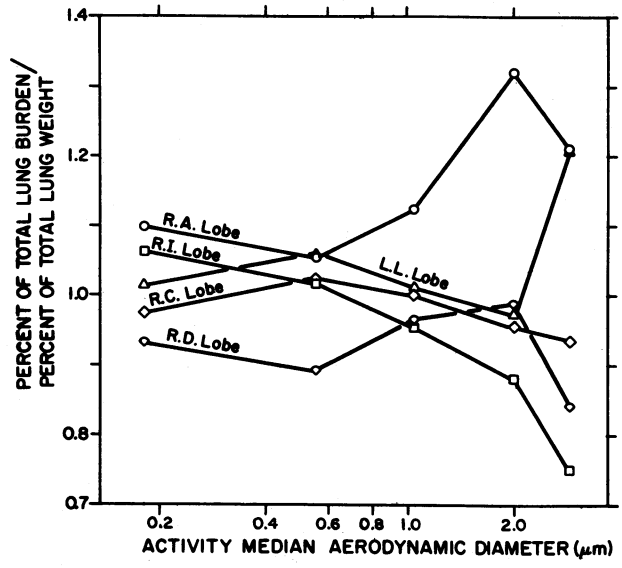

FIGURE 14. Relative lobar concentration of ^{169} Yb in fused aluminosilicate spheres in rats.

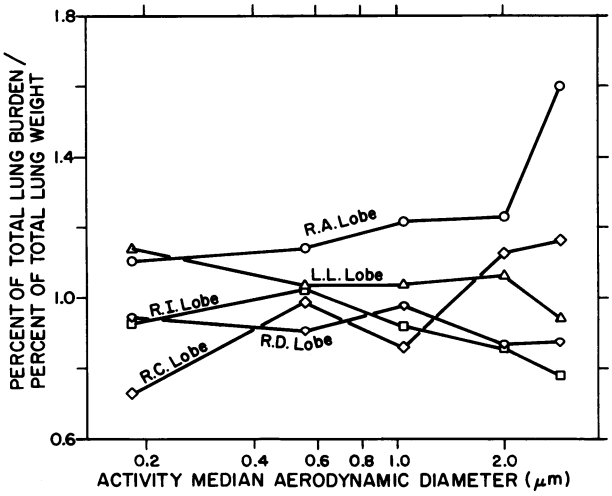

FIGURE 15. Relative lobar concentration of ^{169}Yb in fused aluminosilicate spheres in Syrian hamsters.

spread) among various lobes for smaller particle sizes (except in the case of < 0.2 μm in the hamster), whereas the variation among lobes was larger for larger particle sizes. These phenomena may be partially explained by the variations in the structure of various lobes. As shown in Table 3, the right apical lobe has the smallest number of divisions and shortest path length between the trachea and the terminal bronchioles. This may correlate to the high concentration of deposited particles in this lobe. For decreasing particle size, the particles may reach various lobes more evenly irrespective of the distance. This could explain the reduced spread in relative concentration in these data.

Summary

The initial deposition pattern of inhaled aerosols of radioactive or other toxic materials in man is a major determinant of particle clearance from the respiratory tract, the dose pattern to tissue and resultant biological effect; therefore, it is important in assessing the potential toxicity associated with them. Inhalation deposition of aerosols in the respiratory tract is primarily controlled by: (1) the physics and chemistry of aerosol particles which include the forces acting on inhaled particles and the physical and chemical properties which affect deposition; (2) the anatomy of the respiratory tract which includes such parameters as airway diameters, lengths, and branching angles; and (3) the respiratory physiology which includes air flow in the lung airways and pattern of breathing. Various lung models used to predict particle deposition were reviewed. Also, comparisons of the airway structure of various experimental animals and man were made, showing species differences and lobar difference. Data on the regional deposition of inhaled particles in man, dog, and small rodents were reviewed.

Research supported by the National Institute of Environmental Health Sciences via U.S. Energy Research and Development Administration Contract E(29-2)-1013 under an interagency agreement and conducted in facilities fully accredited by the American Assoication for Accreditation of Laboratory Animal Care.

REFERENCES

1. Findeisen, W. Uber das Absetzen kleiner, in der Luft suspendierten Teilchen in der menschlichen Lunge bei der Atmung. Arch. Gas. Physiol. 236: 367 (1935).
2. Landahl. H. D. On the removal of air-borne droplets by the human respiratory tract. I. The lung. Bull. Math. Biophys. 12:43 (1950).
3. Davies, C. N. A formalized anatomy of the human respiratory tract. In: Inhaled Particles and Vapours, C. N. Davies, Ed., Pergamon Press, New York-London, 1961, p. 82.
4. Weibel E. R. Morphometry of the Human Lung, Academic Press, New York, 1963.
5. Horsfield, K., et al. Models of the human bronchial tract. J. Appl. Physiol. 31: 207 (1971).
6. Granito, S. M. Calculated retention of aerosol particles in the rat lung. Masters Thesis, University of Chicago, 1971.
7. Kliment, V., Libich, J., and Kaudersova, V. Geometry of guinea pig respiratory tract and application of Landahl's model of the deposition of aerosol particles. J. Hyg. Epidemiol. Microbiol. Immunol. 16: 107 (1972).
8. Kliment, V. Similarity and dimensional analysis, evaluation of aerosol deposition in the lungs of laboratory animals and man. Folia Morphol. 21: 59 (1973).
9. Phalen, R. F., et al. Casting the lung *in situ*. Anat. Rec., 177(2): 255 (1973).
10. Davies, C. N. Breathing of half-micron aerosols. II. Interpretation of experimental results. J. Appl. Physiol. 32: 601 (1972).
11. West, J. B. Observations on gas flow in the human bronchial tree. In: Inhaled Particles and Vapours. C. N. Davies, Ed. Pergamon Press, New York-London, 1961, p. 3.
12. Martin, D., and Jacobi, W. Diffusion of small-sized particles in the bronchial tree. Health Phys. 23: 23 (1972).
13. Schroter, R. C., and Sudlow, M. F. Flow patterns in models of the human bronchial airways. Respir. Physiol. 7: 341 (1969).
14. Task Group on Lung Dynamics. Deposition and retention models for internal dosimetry of the human respiratory tract. Health Phys. 12: 173 (1966).
15. Pattle, R. E. The retention of gases and particles in the human nose. In: Inhaled Particles and Vapours, C. N. Davies, Ed. Pergamon Press, New York-London, 1961, p. 302.
16. Gormley, P. G., and Kennedy, M. Diffusion from a stream

flowing through a cylindrical tube. Proc. Roy. Irish Acad. Dublin 52A: 163 (1949).
17. Lippmann, M. Regional deposition of particles in the human respiratory tract. In: Handbook of Physiology, Section on Environmental Physiology. The American Physiological Society, Bethesda, Md., in press.
18. Landahl, H. D. Tracewell, T. N., and Lassen, W. H. On the retention of airborne particulates in the human lung. Arch. Ind. Hyg. Occup. Med. 3: 359 (1951).
19. Landahl, H. D. Tracewell, T. N. and Lassen, W. H. Retention of airborne particulates in the human lung. III. Arch. Ind. Hyg. Occup. Med. 6: 508 (1952).
20. Altshuler, B., et al. Aerosol deposition in the human respiratory tract. Arch. Ind. Health 15: 293 (1957).
21. Muir, D. C. F., and Davies, C. N. The deposition of 0.5 μ diameter aerosol in the lungs of men. Ann. Occup. Hyg. 10: 161 (1967).
22. Giacomelli-Maltoni, G., et al. Deposition efficiency of mono-disperse particulates in human respiratory tract. Amer. Ind. Hyg. Assoc. 33: 603 (1972).
23. Davies, C. N., Heyder, J., and Subba Ramu, M. C. Breathing of half-micron aerosols I. Experimental. J. Appl. Physiol. 32: 591 (1972).
24. Heyder, J. et al. Experimental studies of the total deposition of aerosol particles in the human respiratory tract. J. Aerosol Sci. 4: 191, (1973).
25. Heyder, J., et al. Weitere Untersuchungen zur Deposition von Aerosolsteilchen in menschlichen Atemtrakt. Paper presented at 1973 Congress of the Gesellschaft fur Aerosolforschung at Bad Soden, West Germany, Oct. 18, 1973.
26. Martens, A. and Jacobi, W. Die *in vivo* Bestimmung der Aerosolteilchen Deposition in Atemtrakt bei Mund bzw Nasenatmung. Paper presented at 1973 Congress of the Gesellschaft fur Aerosolforschung, Bad Soden, West Germany Oct. 18, 1973.
27. Lever, J. Cited by C. N. Davies, In Deposition of inhaled particles in man. Chem. Ind. (London) No. 11: 441 (June 1, 1974).
28. Altshuler, B., Palmes, E. D., and Nelson, N. Regional aerosol deposition in the human respiratory tract. In: Inhaled Particles and Vapours. II. C. N. Davies, Ed., Pergamon press, New York-London, 1967, p. 323.
29. Lippmann, M., Albert, R. E., and Peterson, H. T., Jr. The regional deposition of inhaled aerosols in man. In: Inhaled Particles, III, Vol. 1. W. H. Walton, Ed., Unwin Bros., 1971, Old Woking, Surrey, England, p. 105.
30. Cuddihy, R. G., et al. Respiratory tract deposition of inhaled polydisperse aerosols in beagle dogs. J. Aerosol Sci. 4: 35 (1973).
31. Raabe, O. G., et al. Studies of the inhalation deposition of monodisperse aerosols in small rodents. In: Proceedings of the Fourth International Symposium on Inhaled Particles and Vapours. Edinburgh, Scotland, September 22-26, 1975, Pergamon Press, New York-London, in press.